

# Northumbria Research Link

Citation: Yang, Jing-Wen, Wang, Xue-Rui, Zhang, Meng, Xiao, Ling-Yong, Zhu, Wen, Ji, Cai-Shuo and Liu, Cun-Zhi (2018) Acupuncture as a multifunctional neuroprotective therapy ameliorates cognitive impairment in a rat model of vascular dementia: A quantitative iTRAQ proteomics study. *CNS Neuroscience & Therapeutics*, 24 (12). pp. 1264-1274. ISSN 1755-5930

Published by: Wiley

URL: <http://dx.doi.org/10.1111/cns.13063> <<http://dx.doi.org/10.1111/cns.13063>>

This version was downloaded from Northumbria Research Link:  
<http://nrl.northumbria.ac.uk/id/eprint/36090/>

Northumbria University has developed Northumbria Research Link (NRL) to enable users to access the University's research output. Copyright © and moral rights for items on NRL are retained by the individual author(s) and/or other copyright owners. Single copies of full items can be reproduced, displayed or performed, and given to third parties in any format or medium for personal research or study, educational, or not-for-profit purposes without prior permission or charge, provided the authors, title and full bibliographic details are given, as well as a hyperlink and/or URL to the original metadata page. The content must not be changed in any way. Full items must not be sold commercially in any format or medium without formal permission of the copyright holder. The full policy is available online: <http://nrl.northumbria.ac.uk/policies.html>

This document may differ from the final, published version of the research and has been made available online in accordance with publisher policies. To read and/or cite from the published version of the research, please visit the publisher's website (a subscription may be required.)

**ORIGINAL ARTICLE**

# Acupuncture as a multifunctional neuroprotective therapy ameliorates cognitive impairment in a rat model of vascular dementia: A quantitative iTRAQ proteomics study

Jing-Wen Yang<sup>1</sup> | Xue-Rui Wang<sup>2</sup> | Meng Zhang<sup>3</sup> | Ling-Yong Xiao<sup>1</sup> | Wen Zhu<sup>1</sup> | Cai-Shuo Ji<sup>1</sup> | Cun-Zhi Liu<sup>1</sup> 

<sup>1</sup>Department of Acupuncture and Moxibustion, Dongfang Hospital, Beijing University of Chinese Medicine, Beijing, China

<sup>2</sup>Beijing Hospital of Traditional Chinese Medicine affiliated to Capital Medical University, Beijing, China

<sup>3</sup>Department of Applied Sciences, Faculty of Health and Life Sciences, Northumbria University, Newcastle upon Tyne, UK

**Correspondence**

Cun-Zhi Liu, Acupuncture and Moxibustion Department, Beijing Hospital of Traditional Chinese Medicine affiliated to Capital Medical University, Dongcheng District, Beijing, China.  
Email: lcz623780@126.com

**Funding information**

National Natural Science Foundation of China, Grant/Award Number: 81303122

**Summary**

**Aims:** Acupuncture has been reported to affect vascular dementia through a variety of molecular mechanisms. An isobaric tag for relative and absolute quantification (iTRAQ) with high-resolution liquid chromatography-tandem mass spectrometry (LC-MS/MS) analyses makes it possible to attain a global profile of proteins. Hence, we used an iTRAQ-LC-MS/MS strategy to unravel the underlying mechanism of acupuncture.

**Methods:** Wistar rats were subjected to vascular dementia with bilateral common carotid occlusion. Acupuncture was intervened for 2 weeks at 3 days after surgery. The Morris water maze was used to assess the cognitive function. Proteins were screened by quantitative proteomics and analyzed by bioinformatic analysis. Four differentially expressed proteins (DEPs) were validated by western blot. The reactive oxygen species (ROS) production, neuron cell loss, and long-term potentiation (LTP) were determined after western blot.

**Results:** Acupuncture at proper acupoints significantly improved cognitive function. A total of 31 proteins were considered DEPs. Gene ontology (GO) analysis showed that most of the DEPs were related to oxidative stress, apoptosis, and synaptic function, which were regarded as the major cellular processes related to acupuncture effect. Western blot results confirm the credibility of iTRAQ results. Acupuncture could decrease ROS production, increase neural cell survival, and improve LTP, which verified the three major cellular processes.

**Conclusion:** Acupuncture may serve as a promising clinical candidate for the treatment of vascular dementia via regulating oxidative stress, apoptosis, or synaptic functions.

**KEYWORDS**

acupuncture, iTRAQ, proteomics, vascular dementia

## 1 | INTRODUCTION

Vascular dementia (VaD) as the second most common cognitive disorders, following Alzheimer's disease (AD), is caused by a series of

cardiac-cerebral vascular conditions that are characterized by loss of cognitive functions.<sup>1,2</sup> The worldwide number of patients with VaD is estimated to rise because no effective prevention or treatment strategy is available.<sup>3</sup> Progress toward finding effective treatments for VaD

has proved even more elusive than for AD. Cholinesterase inhibitors and memantine as two best studied treatments, both of which are proven therapy for AD, have not been shown to be effective for VaD.<sup>4,5</sup>

Acupuncture is a nonpharmacological therapy that has been extensively tested in patients with VaD in China.<sup>6,7</sup> Several clinical studies have shown therapeutic benefits of acupuncture in patients with VaD.<sup>8,9</sup> However, the molecular events associated with acupuncture are not clearly understood. Acupuncture has been shown to protect cells from the neurotoxicity induced by brain ischemia by exhibiting antioxidative and anti-inflammatory effects or regulating various signaling pathway.<sup>10-13</sup> Given that, there may be not a single or a small amount of protein, but a variety of candidate proteins involved in the acupuncture treatment benefits. Moreover, among the 361 acupoints, ST36 and GV20 are the most commonly used acupoints for the treatment of neurological diseases.<sup>11</sup>

The development of quantitative proteomics technologies using the isobaric labeling strategy has made it possible to obtain global physiological profiles of VaD rats with acupuncture at the protein level. An isobaric tag for relative and absolute quantification (iTRAQ) is a common technique widely used in various areas for simultaneous quantification of 4- or 8-plex samples.<sup>14</sup> The subsequent use of high-resolution liquid chromatography-tandem mass spectrometry (LC-MS/MS) analyses provides accurate relative ratio between protein concentrations, presenting in different samples.<sup>15</sup>

Despite having immense potential to elucidate the underlying mechanism of acupuncture, proteomics studies of VaD treated by acupuncture are lacking. Therefore, this study aims to utilize LC-MS/MS coupled with iTRAQ labeling to identify and quantify the differentially expressed proteins in a VaD rat model. Bioinformatic analysis will be used to select differently expressed proteins related to the mechanisms of acupuncture on rats with VaD. These findings may enhance understanding of the underlying mechanisms of acupuncture on VaD.

## 2 | MATERIALS AND METHODS

### 2.1 | Animals

Eight-week-old male Wistar rats (280-320 g, housed under 12-hours light and dark conditions with food and water available ad libitum) were used in this study. All animals were provided by the Vital River Laboratory Animal Technology Co., Ltd (Beijing, China). This study was carried out in accordance with the recommendations of the Guide for the Care and Use of Laboratory Animals and approved by the Ethics Committee for Animal Experimentation and Use Committee of China Academy of Chinese Medical Sciences.

### 2.2 | Experimental design

#### 2.2.1 | Experiment 1

To compare the effect of acupuncture at proper acupoints on the cognitive deficits with that of placebo acupuncture (the same

stimulation was applied to a non-acupoint) in a vascular dementia model, we randomly divided 24 rats into 4 groups: sham, 2VO (model only), Acu (model with acupuncture at proper acupoint), and Non-acu (model with acupuncture at a non-acupoint).

#### 2.2.2 | Experiment 2

To determine the beneficial effect of acupuncture in the hippocampus of vascular dementia rats at protein level, we divided a further 18 rats (n = 6 each group) into 3 groups: sham, 2VO, and Acu.

#### 2.2.3 | Experiment 3

To verify the beneficial effect of acupuncture which was confirmed by iTRAQ-based proteomics, we divided a further 18 rats (n = 6 each group) into 3 groups: sham, 2VO, and Acu.

#### 2.2.4 | Experiment 4

To clarify the role of S100b in acupuncture neuroprotective effect, we divided a further 24 rats (n = 6 each group) into 4 groups: 2VO, Acu, 2VO +S100b siRNA, and 2VO +Control siRNA.

### 2.3 | Bilateral common carotid arteries occlusion

Bilateral surgical ligation of the common carotid arteries (2-vessel occlusion, 2VO) in rats remains the most frequently used model of vascular dementia.<sup>16,17</sup> Rats were anesthetized intraperitoneally with 2.5% pentobarbital sodium (50 mg/kg). The bilateral common carotid arteries were exposed and then ligated with 5-0 silk sutures. In the sham group, the same operations were performed without artery occlusion.

### 2.4 | Acupuncture treatment

Three days after surgery, acupuncture was performed at ST36 and GV20 (Acu) or at non-acupoint (Non-acu) once daily for 14 days (1 day rest after 6 days treatment). Sterilized disposable needles (0.3 × 40 mm, Hwato, China) were selected to stimulate ST36 and GV20 or non-acupoints, and the location and the operated method of acupoints are shown in Table 1. The rats in the sham and 2VO group were given the same account catching-grasping stimulus without the acupuncture stimulation.

### 2.5 | Morris water maze (MWM)

To assess spatial learning and memory, rats were trained and tested in MWM after acupuncture as described before.<sup>18</sup> In brief, each rat was trained 3 times per day for 5 consecutive days. The rat was free to swim until it found the platform or was guided in place if the animal does not reach the platform during 90 seconds. Before removed from the pool, each rat was placed on the platform for 10 seconds. On day 6, the hidden platform was removed and the

**TABLE 1** Acupuncture points and manipulations

| Points         | Anatomical positions   | Manipulation                               | Twisting angle (degrees) | Frequency (per minutes) | Time (s) |
|----------------|--|--|--------------------------|-------------------------|----------|
| Zusanli (ST36) | 2 mm lateral to the anterior tubercle of the tibia and 5 mm below the capitulum fibulae under knee joint | Twirling reinforcing manipulation          | <90                      | >120                    | 30       |
| Baihui (DU20)  | Midline of the head, approximately midway on the line connecting the apices of the auricles              | Twirling reinforcing manipulation          | <90                      | >120                    | 30       |
| Non-acupoints  | On the bilateral hypochondrium, 10 mm above iliac crest  | Moderate reinforcing-reducing manipulation | 90-180                   | 60-120                  | 45       |

rats were allowed to swim freely for 90 seconds. We recorded the quadrant dwell time in the target quadrant and calculated it by the computer with a tracking system (TopScan Lite Animal Behavior Analysis System, USA).

## 2.6 | Electrophysiological recordings

Rats were fixed with a stereotaxic frame (SR-6 N; Narishige, Japan) after anesthetized with urethane (1.2 g/kg, IP). Electrodes were positioned as our previous study.<sup>18</sup> The lateral prepenetrating (PP) was stimulated during the long-term potentiation (LTP) experiments. After a 30-minute stable baseline recording, LTP was induced by high-frequency stimulation consisting of 4 trains of 30 stimuli applied at 500 Hz with an intertrain interval of 10 seconds. After tetanic stimulation, the field excitatory postsynaptic potential (fEPSP) was recorded for 60 minutes, and the fEPSP slope level was present by the ratio of absolute of fEPSP slope to baseline value.

## 2.7 | Sample collection

At the termination of the experiment, rats were euthanized with a sodium pentobarbital overdose (100 mg/kg). The brains were removed, and the hippocampi were dissociated for protein extraction and proteomics analysis. The remaining brains were sectioned and were immersed in 4% paraformaldehyde to fix for histopathologic evaluation.

## 2.8 | iTRAQ-based quantitative proteomic analyses

In this experiment, there were three groups of rats ( $n = 6$  per group) to evaluate the proteome regulated by ischemia and acupuncture. Each group contained six hippocampus isolated from different animals to minimize the surgical and biological variations between individual subjects.

### 2.8.1 | Sample preparation

Frozen tissues from hippocampus were ground and suspended in freshly prepared 10% TCA in 0.2% DTT-containing acetone. After 30 minutes centrifugation at 20 000 g at 4°C, the pellet was collected

and resuspended in 1.3 mL of 0.2% DTT in acetone, then centrifugation for 30 minutes at 20 000 g at -20°C. After dissolved in 8 mol/L urea with protease inhibitor cocktail (Roche, Germany), the pellets were intermittent sonication for 20 seconds, followed by centrifuged to collect the supernatant. DTT was added to the supernatant to a final concentration of 10 mmol/L and then water bathed for 1 hour. After that, iodoacetamide was rapidly added to a final concentration of 55 mmol/L followed by standing in the dark for 1 hour. The proteins mixture was purified by adding 4-fold volume cold acetone and left at -20°C for 3 hours. The precipitated proteins were collected by centrifuging at 20 000 × g at 4°C for 30 minutes followed by dissolving in the reconstitution buffer containing 50% TEAB and 0.1% SDS. Protein contents were assayed by the Bradford assay.

### 2.8.2 | Protein digestion and peptide iTRAQ labeling

Samples (100 µg of proteins/condition) were digested with 3.3 µg trypsin for 24 hours at 37°C and then digested for another 12 hours with a supplementary 1 µg trypsin. The peptides were vacuum centrifuged to dryness. Following trypsin digestion, the peptides were reconstituted and individually labeled with 8-plex iTRAQ reagents (Applied Biosystems, USA) as follows: sham group (115 tag), 2VO group (118 tag), and Acu group (113 tag). The labeled peptides were combined and dried in a vacuum centrifuge.

### 2.8.3 | Strong cation exchange (SCX) Chromatography

The peptides were dried and reconstituted in Buffer A (10 mmol/L KH<sub>2</sub>PO<sub>4</sub> in 25% ACN; pH 3.0) and fractionated using a Phenomenex HPLC Luna SCX column (150\*4.6 mm; 5 µm; 100 Å) (PolyLC, Columbia, MD). Then, a 76-min gradient was adopted with Buffer B (10 mmol/L KH<sub>2</sub>PO<sub>4</sub> and 2 mol/L KCl in 25% ACN; pH 3.0) to elute the peptides. The elution fractions were collected at 1-min intervals and pooled into 16 fractions.

### 2.8.4 | LC and MS/MS analyses

The reconstituted peptides were analyzed with the Q-Exactive mass spectrometer (Thermo Fisher Scientific, Waltham, MA, USA) coupled

with a nano high-performance liquid chromatography (UltiMate 3000 LC Dionex; Thermo Fisher Scientific) system. The iTRAQ-labeled peptides were separated on a home-packed nanobored C18 column with a picofrit nanospray tip (75  $\mu$ m ID \* 15 cm, 5  $\mu$ m particles) using mobile phase A (0.1% FA in 2% ACN) and phase B (0.1% FA in 100% ACN). The Q-Exactive was used with high energy collision dissociation (HCD) in each MS and MS/MS cycle. MS spectra were collected in the range 350-2000 m/z at a resolving power of 70 000. The automatic gain control (AGC) target was set to  $3 \times 10^6$ , and the maximum ion time was 50 ms MS/MS analyses were set at a resolving power of 17 500 with a maximum ion time of 100 ms and a normalized collision energy of 28. Precursor ions were excluded from reselection for 15 seconds.

## 2.8.5 | Proteomic data analysis and bioinformatics

The raw mass data were processed for the peptide data analysis using Proteome Discoverer 1.4 (ver. 1.4.0.288; Thermo Fisher Scientific) with a false discovery rate ( $FDR = N(\text{decoy})^2 / (N(\text{decoy}) + N(\text{target}))$ ) <1% and expected cutoff or ion score <0.05 (with 95% confidence) for searching the Uniprot\_2015\_rattus database. Protein probabilities were assigned using the Protein Prophet algorithm, and proteins with at least two unique peptides were identified. The upregulated or downregulated proteins in all replicates with relative quantification *P*-values <0.05-fold and 1.2-fold changes were selected as being differentially expressed in the data. The following options were used to identify the proteins: peptide mass tolerance =  $\pm 15$  ppm, MS/MS tolerance = 20 mmu, enzyme = trypsin, missed cleavage = 1, fixed modification: carbamidomethyl (C), variable modification: oxidation (M), Gln $\rightarrow$ Pyro-Glu (N-termQ), iTRAQ 8plex (K), iTRAQ 8plex (Y), and iTRAQ 8plex (N-term), database pattern = decoy.

Gene ontology (GO) was performed using the bioinformatics analysis tool DAVID (<https://david.abcc.ncifcrf.gov>) to determine the functional classifications of the identified proteins. The interactions among these proteins regarding the biological pathways were determined using Pathway Studio software and the Kyoto Encyclopedia of Genes and Genomes (KEGG) database to better understand these differentially expressed proteins in relation to the published literature. Significant pathway enrichment was defined as a corrected FDR of  $P < 0.05$ .

## 2.9 | Western blotting validation

Western blot analyses were performed to validate the proteomics results.<sup>19</sup> The protein samples were separated by 10% SDS-PAGE gels and transferred to PVDF membranes. The membranes were blocked with 5% non-fat milk in TBS and then incubated overnight at 4°C with primary antibodies, including antibodies against S100-B (S100B), copper chaperone for superoxide dismutase (SOD1), 14-3-3 protein epsilon (14-3-3e), high mobility group protein B1 (HMGB1), and  $\beta$ -actin (both at 1:1000; Abcam, USA). The membranes were then washed and incubated for 1 hour at room temperature with secondary antibodies (1:5000; Abcam, USA), and the images were captured using the Odyssey Infrared Imaging System (LI-COR Biosciences, Nebraska USA).

## 2.10 | Nissl staining and dihydroethidium (DHE) staining

We used a cryostat to section the frozen tissues to a thickness of 20  $\mu$ m. The slides were immersed in 0.2% cresyl violet solution for 30 minutes at 37°C followed by covered with a xylene-based mounting medium. Another investigator who was blinded observed the sections by a light microscope (Olympus).

Frozen sections were loaded with 5  $\mu$ mol/L DHE (Molecular Probes) at 37°C for 60 minutes. Reactive oxygen species (ROS) fluorescence was measured by a DM 6000 B fluorescence microscope (Leica, Germany) at excitation 515 nm and emission 585 nm. Data were analyzed by the Fluoview software (Olympus).

## 2.11 | Microinjection into intracerebroventricular

S100b siRNA was purchased from GenePharma China Ltd (Shanghai, China). The sense and antisense primer of S100b is as follows: 5'-GCC CUC AUU GAU GUC UUC CAC CAG U-3' and 5'-ACU GGU GGA AGA CAU CAA UGA GGG C-3', respectively. The negative siRNA was used as the control siRNA. Rats were anesthetized with sodium pentobarbital (40 mg/kg intraperitoneally) and fixed in a stereotaxic apparatus (Stoelting Co, IL, USA). S100b siRNA or control siRNA (1  $\mu$ g/ $\mu$ L; 10  $\mu$ L) was injected into the ipsilateral lateral ventricle (-1 mm anteroposterior, 2 mm lateral, 4 mm deep). The location was confirmed by pontamine sky blue (0.2%, 1  $\mu$ L) microinjection after completion of the experiments.

## 2.12 | Data and statistical analyses

We carried out statistical analyses with SPSS 17.0 software. All data were expressed as mean  $\pm$  SEM. The Morris data were analyzed by 2-way repeated-measures ANOVA. The other values were analyzed by 1-way ANOVA, followed by a post hoc Tukey's test. The significance level was set as  $P < 0.05$ .

# 3 | RESULTS

## 3.1 | Acupuncture improves cognitive functions in VaD rats

We examined spatial learning and memory in the MWM to test the hypothesis that acupuncture at proper acupoint not non-acupoint could improve cognitive function of VaD rats. As shown in Figure 1, rats subjected to 2VO and treated with acupuncture at non-acupoint needed much more time to find the hidden platform (escape latency) compared with the sham rats. In contrast, the escape latency was significantly shortened by acupuncture as compared to the 2VO group (Figure 1A,  $P < 0.01$ ). Swim speed was unaffected by surgery or acupuncture, illustrating that four group rats had equivalent motor skills (Figure 1B,  $P > 0.05$ ). In the probe trial, 2VO rats showed a shorter time in the target quadrant compared to the sham group. However, the decreased time in 2VO group was significantly increased by acupuncture. Significant differences were found between the Acu and

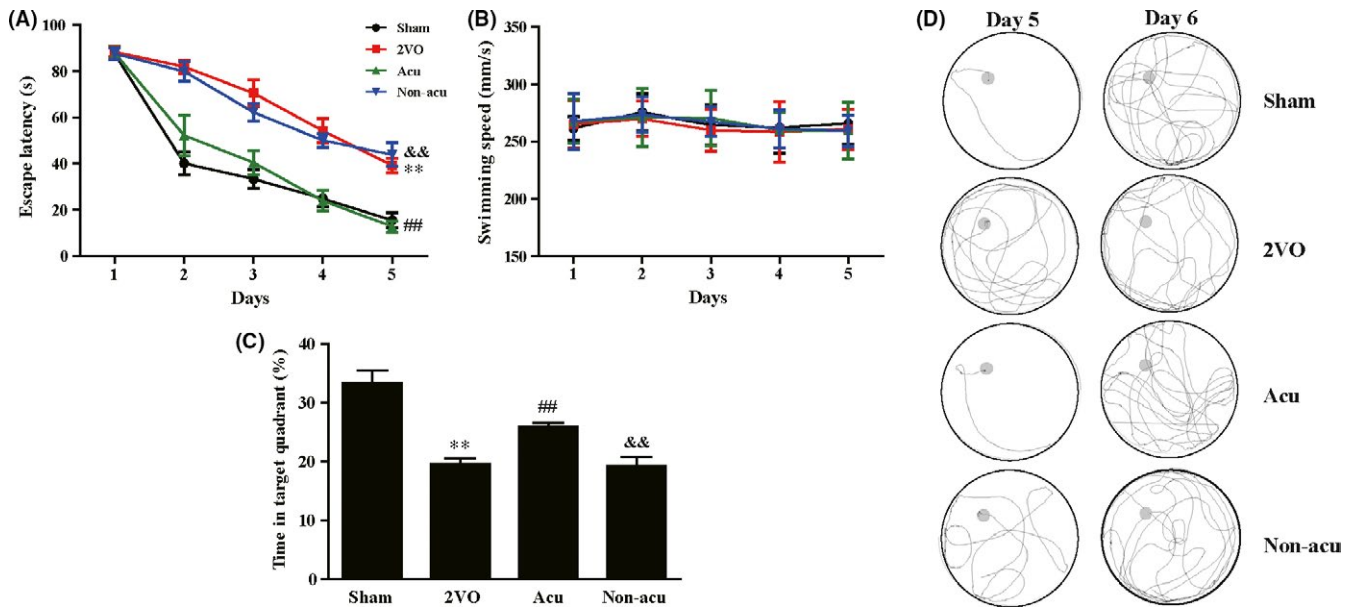


**FIGURE 1** Acupuncture improves cognitive functions in VaD rats. Quantification of A, escape latency; B, swimming speed for reaching the hidden platform during 5 days in hidden platform trial, and C, the percentage of time spent in the target quadrant in probe trial was measured in sham, 2VO, Acu, and Non-acu rats using water maze task. Values are expressed as means  $\pm$  SEM ( $n = 6$  for each group). D, Typical swimming traces of all groups on day 5 and 6. \* and \*\* indicate  $P < 0.05$  and  $P < 0.01$ , respectively, compared with the sham group; # and ## indicate  $P < 0.05$  and  $P < 0.01$ , respectively, compared with 2VO group; & and && indicate  $P < 0.05$  and  $P < 0.01$ , respectively, compared with Acu group

Non-acu groups (Figure 1C,  $P < 0.01$ ). Figure 1D shows representative diagrams of search trajectories in MWM.

Taken together, these results demonstrated that acupuncture at proper acupoint could ameliorate the behavioral impairment specifically. Considering the specificity of acupoint effects has been confirmed, we used the sham, 2VO, and Acu group in the following experiments.

### 3.2 | Characterization of molecular events involved in neuroprotection by iTRAQ-based quantitative proteomic analyses

#### 3.2.1 | Identification of differentially expressed proteins

After analyzed as described in the method, a total of 1789 non-redundant proteins were confidently identified (Data S1). Proteins were considered differentially expressed when the expression ratios more than 1.2-fold changes while  $P$ -value less than 0.05. In total, there were 221 quantified proteins considered differentially expressed (Data S2), with 31 differentially expressed proteins (DEPs) appearing in the two comparisons (2VO group vs sham group and Acu group vs 2VO group) (Table 2).

#### 3.2.2 | Bioinformatics analysis

As shown in Figure 2, the significantly enriched functional terms were performed by a GO analysis. GO analysis consists of three components:

cellular components (GO-CC), biological processes (GO-BP), and molecular functions (GO-MF). GO-CC reflected DEPs distributed in different cell components. In our study, proteins localized in the extracellular exosome had the highest -LgP score (Figure 2A). GO-MF showed that proteins related to protein binding and metal ion binding were most common (Figure 2B). GO-BP demonstrated that the oxidation-reduction process and synaptic transmission were the most heavily interfered biological processes (Figure 2C). Among the biological processes, we found most of them related to oxidative stress, apoptosis, or synaptic function, which have been defined as the major processes related to acupuncture effect. Therefore, we conducted a Venn diagram to find key proteins overlapping among the processes (Figure 2E).

We further analyzed the biological function of DEPs by using the KEGG database and mapped them to 54 pathways. The most enriched pathways are shown in Figure 2D, including neurodegeneration disease, dopaminergic synapse, oxidative phosphorylation, long-term potentiation, etc

### 3.3 | Validation of iTRAQ-based proteomics results

Four DEPs, namely S100B, SOD1, 14-3-3e, and HMGB1, were chosen for further validation using western blot (Figure 3). S100B, HMGB1, and 14-3-3e expressions were markedly upregulated in 2VO rats compared to sham rats. Acupuncture notably suppressed the upregulation of S100B and HMGB1. In contrast, the expression level of 14-3-3e was also dramatically increased after acupuncture. SOD1 was markedly downregulated in the 2VO rats in comparison with the sham rats. Acupuncture caused a reversal in the expression of SOD1. Taken



**TABLE 2** Dysregulated proteins

| Accession | Protein name  | Function | 2VO/Sham     | Acu/2VO      |
|-----------|---|----------|--------------|--------------|
| Q9JK72    | Copper chaperone for superoxide dismutase                       | a        | 0.762        | <b>1.493</b> |
| O35431    | Amyloid beta A4 precursor protein-binding family A member 2     | c        | <b>1.475</b> | 0.637        |
| P08753    | Guanine nucleotide-binding protein G(k) subunit alpha           | c        | <b>1.445</b> | 0.767        |
| Q6PCT8    | Succinate dehydrogenase [ubiquinone] cytochrome b small subunit | a        | <b>1.374</b> | 0.784        |
| P14056    | Serine/threonine-protein kinase A-Raf                           | b        | <b>1.347</b> | 0.744        |
| Q9ES40    | PRA1 family protein 3   | a,b      | <b>1.264</b> | 0.77         |
| P61295    | Heart and neural crest derivatives-expressed protein 2          | b        | <b>1.261</b> | <b>1.324</b> |
| P62078    | Mitochondrial import inner membrane translocase subunit Tim8 B  | d        | <b>1.227</b> | 0.757        |
| Q5XIM4    | ATP synthase subunits, mitochondrial                            | d        | <b>1.223</b> | 0.786        |
| Q5PQJ6    | Pyrroline-5-carboxylate reductase 3                             | a        | <b>1.216</b> | <b>1.411</b> |
| Q63707    | Dihydroorotate dehydrogenase (quinone), mitochondrial           | a,b      | <b>1.216</b> | <b>1.224</b> |
| Q9JLH7    | CDK5 regulatory subunit-associated protein 3                    | c        | <b>1.211</b> | <b>1.301</b> |
| P04631    | Protein S100-B  | a,b,cc   | <b>1.209</b> | 0.798        |
| P62260    | 14-3-3 protein epsilon  | b,c      | <b>1.206</b> | <b>1.846</b> |
| Q05962    | ADP/ATP translocase 1   | b        | <b>1.203</b> | 0.783        |
| Q62760    | Mitochondrial import receptor subunit TOM20 homolog             | d        | <b>1.201</b> | <b>1.226</b> |
| Q9WV97    | Mitochondrial import inner membrane translocase subunit Tim9    | d        | 0.791        | 0.733        |
| Q00959    | Glutamate receptor ionotropic, NMDA 2A                          | c        | 0.782        | <b>1.254</b> |
| P07171    | Calbindin   | c        | 0.772        | <b>1.347</b> |
| P60570    | Pannexin 1  | d        | 0.76         | <b>1.873</b> |
| Q9Z1W6    | Protein LYRIC   | b        | 0.75         | <b>1.237</b> |
| Q8R4A1    | ERO1-like protein alpha   | a        | 0.749        | <b>1.224</b> |
| Q8VGC3    | Voltage-dependent L-type calcium channel subunit beta-2         | c        | 0.744        | <b>1.404</b> |
| Q66H15    | Regulator of microtubule dynamics protein 3                     | b,c      | 0.724        | <b>1.358</b> |
| P60905    | DnaJ homolog subfamily C member 5                               | b,c      | 0.721        | <b>1.216</b> |
| P86173    | Actin-like protein 6B   | c        | 0.706        | <b>1.368</b> |
| P63025    | Vesicle-associated membrane protein 3                           | c        | 0.68         | <b>1.944</b> |
| P04937    | Fibronectin   | b,c      | 0.632        | <b>2.584</b> |
| P63159    | High mobility group protein B1                                  | b,c      | <b>1.243</b> | 0.618        |
| Q3MHU3    | Putative ATP-dependent RNA helicase TDRD9                       | d        | 0.602        | <b>3.406</b> |
| P10960    | Sulfated glycoprotein 1   | b        | 0.571        | <b>1.351</b> |

Overall upregulation was labeled in bold; overall downregulation was labeled in italics.

<sup>a</sup>Proteins involved in angiogenesis.

<sup>b</sup>Proteins involved in neurogenesis and synaptogenesis.

<sup>c</sup>Proteins involved in inflammation.

<sup>d</sup>Proteins involved in reactive astrocytosis.

together, western blot results confirm the consistency between the two approaches, despite slight differences between the mean values.

### 3.4 | Validation of molecular events

Bioinformatics analysis showed that oxidative stress, apoptosis, and synaptic function are the major processes related to acupuncture effect. To verify the three processes, we used DHE staining, Nissl staining, and electrophysiology to test ROS production, neuron apoptosis, and LTP, respectively (Figure 4). Compared to the sham rats, 2VO rats showed overproduction ROS, less surviving

neurons, and impaired synaptic function. Acupuncture decreased ROS production, increased number of neuron, and enhanced LTP ( $P < 0.05$ ).

### 3.5 | Validation of the protein-specific effects via used siRNA

Our results have shown that S100b is a key protein regulating three major processes, so we choose it to verify its relationship with cognitive function. S100b siRNA was microinjected into rat lateral ventricle followed by Morris water maze. As shown in

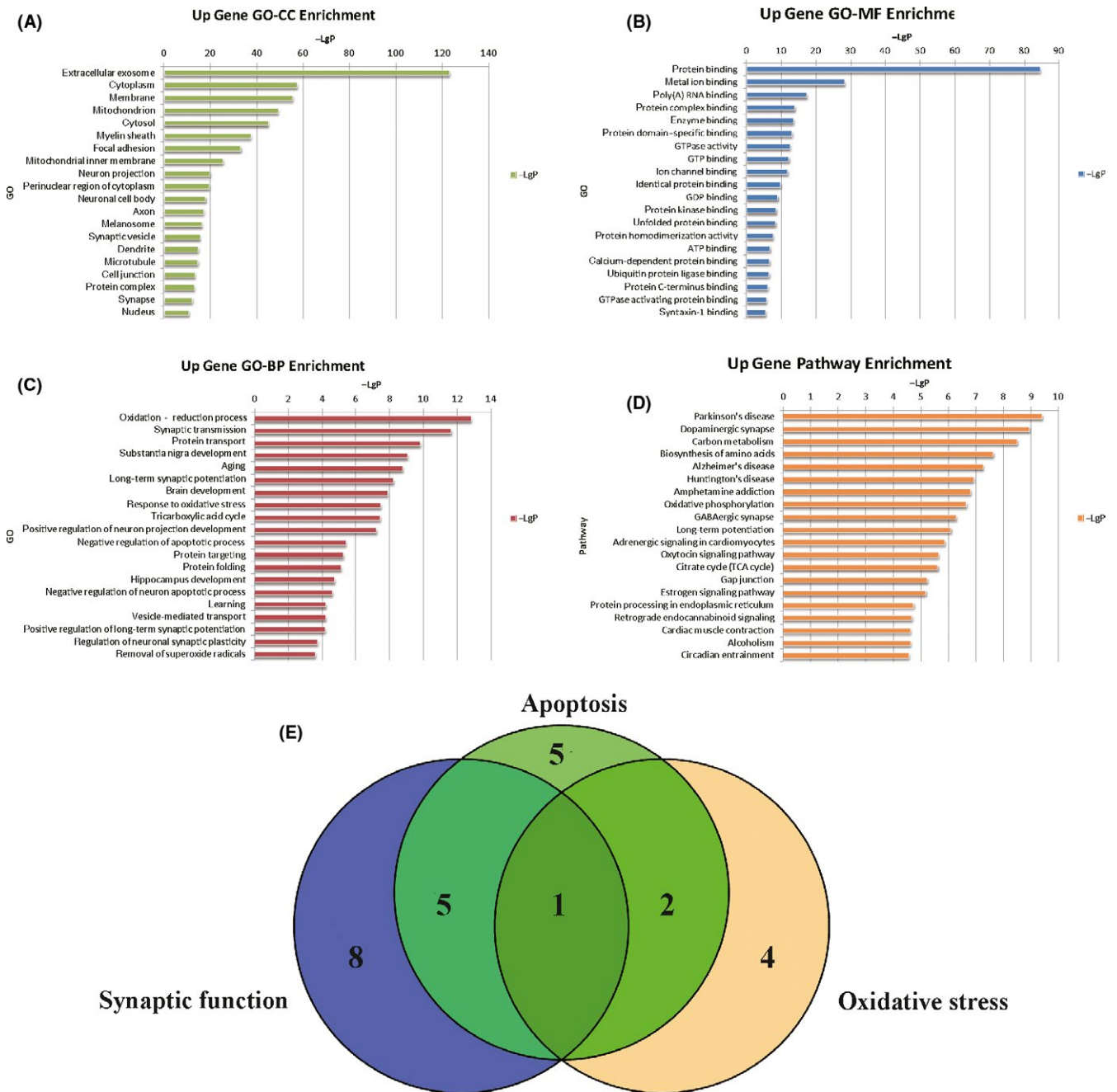


**FIGURE 2** Characterization of molecular events involved in neuroprotection by iTRAQ-based quantitative proteomic analyses. All identified proteins were functionally annotated in GO database A-C, according to their biological process, cellular component, and molecular function. D, All identified proteins were functionally annotated in KEGG database. E, Dysregulated proteins functionally annotate to cellular processes of oxidative stress, apoptosis, and synaptic function

Figures 5 and 6, compared with the 2VO group, the escape latency was reduced in the Acu and 2VO+S100b siRNA group ( $P < 0.05$ ), and the time spent in the target quadrant increased significantly ( $P < 0.05$ ). The escape latency was prolonged significantly in the 2VO+Control siRNA group in comparison with the Acu and 2VO+S100b siRNA group. Besides, the time spent in the target quadrant was decreased in the 2VO + Control siRNA group ( $P < 0.05$ ). No significant changes were found between the 2VO group and the 2VO+ Control siRNA group ( $P > 0.05$ ).

## 4 | DISCUSSION

VaD is one of the most common causes of dementia after AD and is described as having problems with reasoning, planning, judgment, and memory caused by impaired blood flow to the brain. However, unlike AD, there are no licensed treatments for VaD.<sup>20,21</sup> In this study, acupuncture at proper acupoint effectively reduced escape latency by 56.3%-67.08% reduction. Then, we used iTRAQ-based quantitative proteomic analyses to elucidate the molecular events



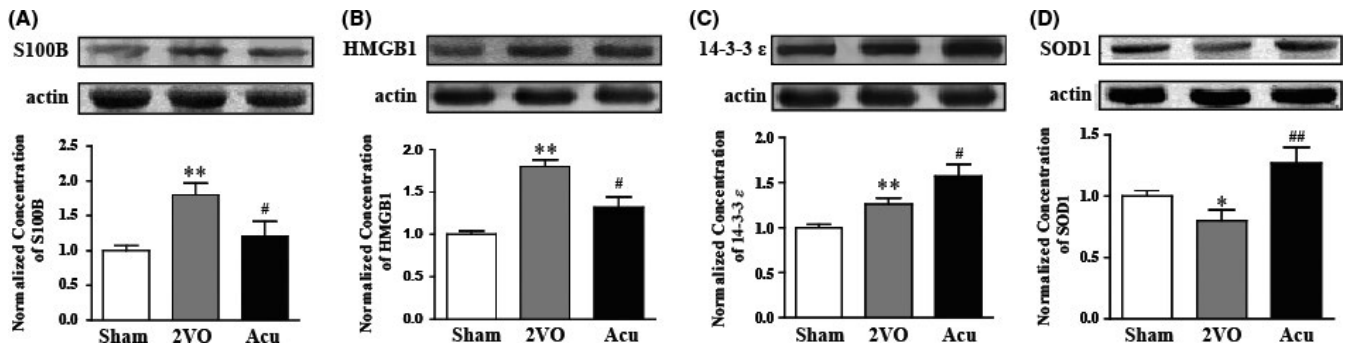


**FIGURE 3** Western blot analysis to verify selected differentially expressed proteins. Candidate proteins were examined and normalized to  $\beta$ -actin levels ( $n = 6$ , hippocampus). \* and \*\* indicate  $P < 0.05$  and  $P < 0.01$ , respectively, compared with the sham group; # and ## indicate  $P < 0.05$  and  $P < 0.01$ , respectively, compared with 2VO group

involved in the beneficial effect of acupuncture. To our knowledge, this is the first comparative proteomic study to explore the mechanisms of acupuncture in VaD rats at protein level. In total, we identified 31 DEPs which are susceptible to ischemic injury and acupuncture simultaneously—most of them involved in oxidative stress, apoptosis, and synaptic function.

Numerous clinical and animal studies have demonstrated that acupuncture could improve learning and memory ability.<sup>22-24</sup> In

our experiments, acupuncture at proper acupoint not non-acupoint improved spatial learning and memory ability of VaD rats, which indicated that the effect of acupuncture has acupoint specificity. However, the explicit mechanism of acupuncture in treating VaD is unclear. In VaD, chronic hypoperfusion leads to a decrease in cerebral blood flow, hypoxia, and oxidative stress and triggers inflammatory responses. Hypoxia-induced oxidative stress leads to mitochondrial dysfunction, microglial activation, neuronal damage, and apoptosis

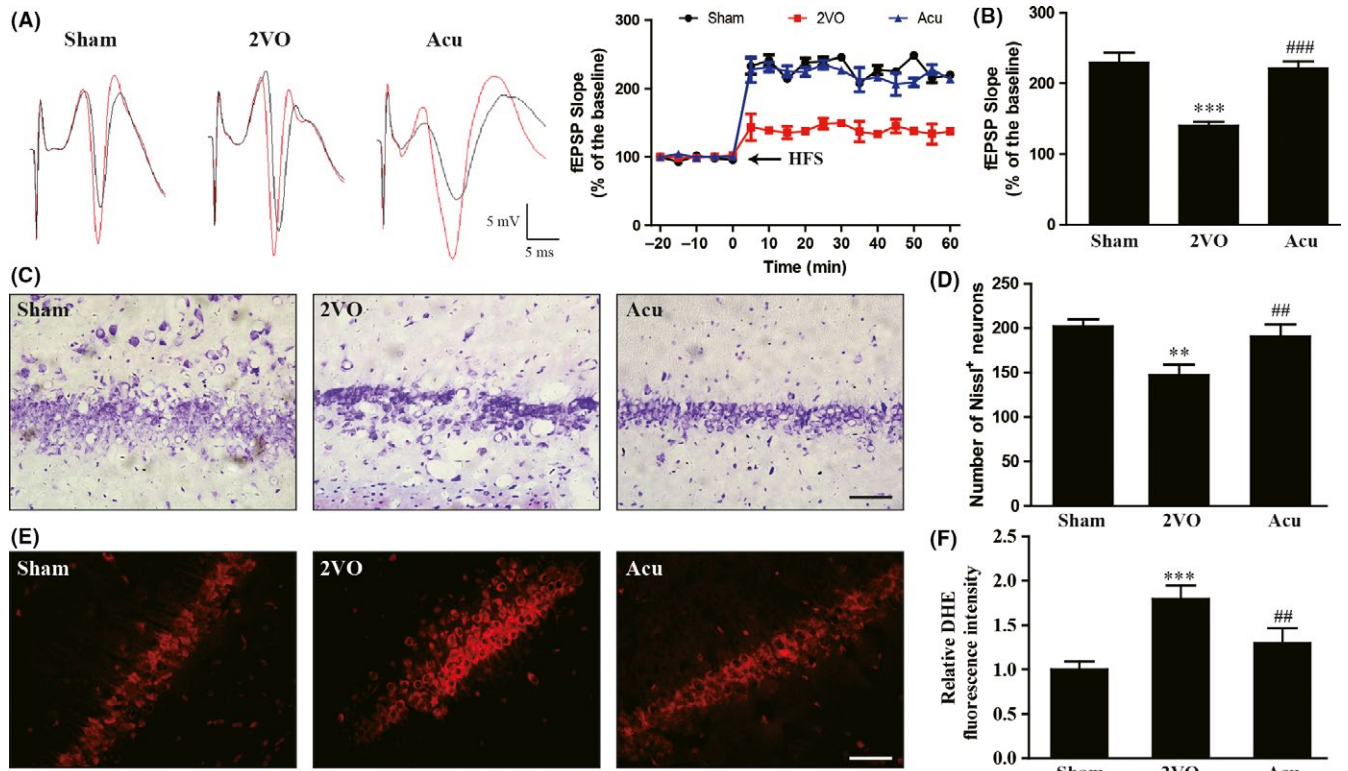


**FIGURE 4** Molecular and cellular events involved in the protection of acupuncture against ischemic injury. A, 2VO strongly inhibited the induction of LTP, and acupuncture reversed the inhibition. B, The evoked synaptic responses were summarized by calculating the average of field excitatory postsynaptic potential (fEPSP) slope 5–60 min after high-frequency stimulation (HFS). C, Representative images of Nissl staining (hippocampus CA1 area). Scale bars, 50  $\mu$ m. D, Quantification of the number of Nissl positive neurons. E, Representative images of DHE staining (hippocampus CA1 area). Scale bars, 50  $\mu$ m. F, Quantification of fluorescence intensity of the DHE channel.  $n = 6$ . \*\* and \*\*\* indicate  $P < 0.01$  and  $P < 0.001$ , respectively, compared with the sham group; ## and ### indicate  $P < 0.01$  and  $P < 0.001$ , respectively, compared with 2VO groups

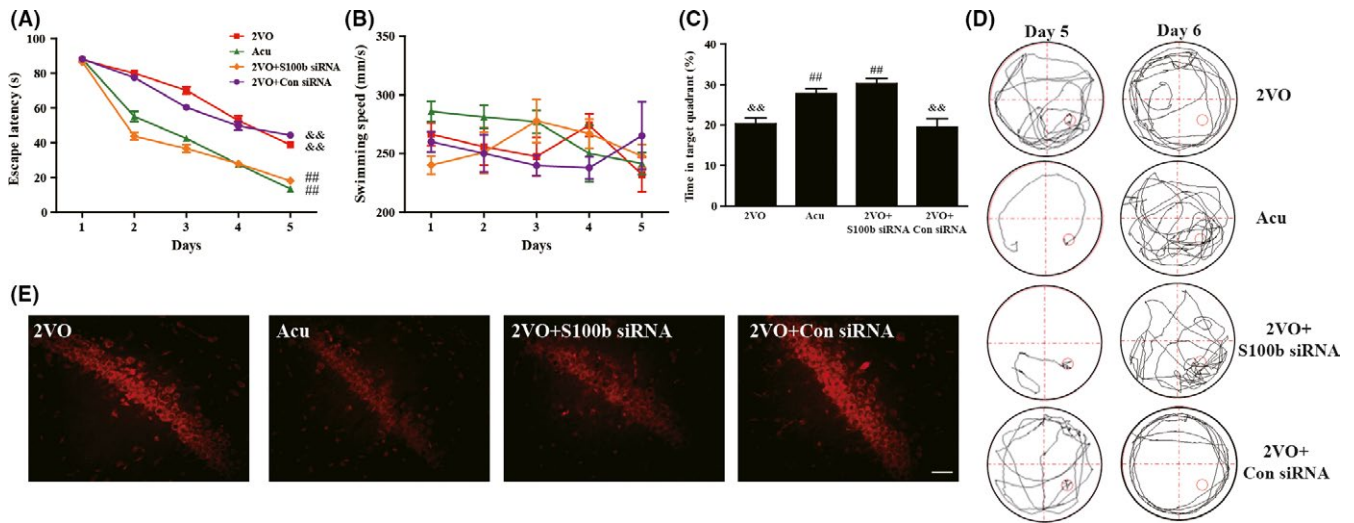


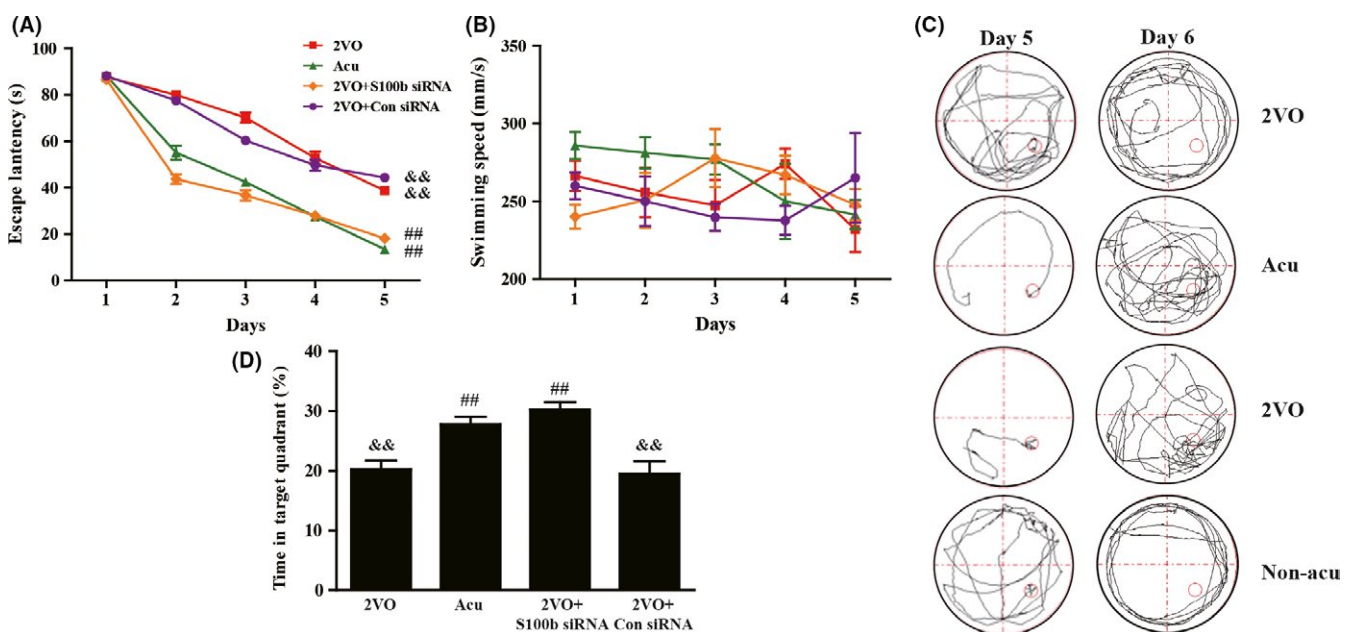
**FIGURE 5** S100B siRNA injection mimicked the antioxidant and neuroprotective potential of acupuncture. Quantification of A, escape latency; B, swimming speed for reaching the hidden platform during 5 days in hidden platform trial, and C, the percentage of time spent in the target quadrant in probe trial was measured in 2VO, Acu, 2VO+S100b siRNA, and 2VO+Control siRNA rats using MWM. Values are expressed as means  $\pm$  SEM (n = 6 for each group). D, Typical swimming traces of all groups on day 5 and 6. E, Representative images of DHE staining (hippocampus CA1 area). ## indicate  $P < 0.01$  compared with 2VO group; && indicate  $P < 0.01$  compared with Acu group

via multiple signal pathways.<sup>25</sup> The hippocampus, as the core for spatial learning and memory, is highly susceptible to hypoperfusion-induced lesions. Our previous study proved that acupuncture could activate the antioxidant effects or reverse hippocampal mitochondrial dysfunction to prevent spatial memory deficits.<sup>26,27</sup> The major cellular processes observed in our proteomic changes were associated with oxidative stress, apoptosis, and synaptic functions, revealing that acupuncture possibly regulates the brain tissue repair via regulating oxidative stress, apoptosis, or synaptic functions.

One of the main causes of VaD-induced cognitive deficits is the oxidative stress stimulated by the disruption of cerebral blood flow.<sup>28</sup>

Oxidative stress reflects an imbalance between the overproduction of ROS and antioxidants. SOD1, one of the most common antioxidants, has an ability to remove ROS, which is often inhibited during ischemic injury.<sup>29,30</sup> It means antioxidant activity is far from enough to completely remove excess ROS. Lin and his colleagues demonstrated that acupuncture could ameliorate learning and memory in rats with ischemic injury via increasing the activity of SOD1,<sup>31</sup> which is consistent with our results.

Overgeneration of ROS can cause cell death and apoptosis of neurons leading to permanent neuronal damage. HMGB1 is important for oxidative stress response and cell death signaling. HMGB1 has been shown to play an important role in signaling for



mitochondrial dysfunction-induced apoptosis.<sup>32</sup> Ding et al reported that the HMGB1 together with its receptor Toll-like receptor 4 plays a significant role in the pathogenesis of ischemic-reperfusion injury and can induce apoptosis.<sup>33</sup> In the present study, acupuncture could reverse the expression of HMGB1 and play a role of anti-apoptotic.

The hippocampus and prefrontal cortex are the most important brain regions in the formation of learning and memory. As the part of a brain system responsible for learning and memory, hippocampus is very sensitive to ischemic injury. Learning is widely believed to involve synaptic plasticity, employing mechanisms such as those used in long-term potentiation (LTP) and long-term depression (LTD). It is well accepted that the induction of LTP requires activation of postsynaptic N-methyl-D-aspartic acid (NMDA) receptors during postsynaptic depolarization. This results in a rise in Ca<sup>2+</sup> concentration, a necessary trigger for LTP.<sup>34</sup> In our experiment, the expression of NMDA 2A receptor was increased after acupuncture treatment, which may be associated with the beneficial effect of acupuncture on cognitive function. Voltage-dependent L-type calcium (Ca) channels (VDCCs), as one of the DEPs, are heteromultimeric proteins that are regulated through phosphorylation by cAMP-dependent protein kinase (PKA). In addition, VDCCs have been reported to play a critical role in neurotransmitter release evoked by nnAChR activation, and participate in memory facilitation; 14-3-3 is a family of regulatory proteins enriched at the synapse and plays a positive role in learning, memory, and synaptic plasticity. Simsek-Duran et al reported that 14-3-3 is necessary for the presynaptic form of LTP.<sup>35</sup> In this study, we found that 2VO rats had hippocampal-dependent learning and memory deficits, and the deficits may be due to the changes in synaptic ultrastructure, dendritic spine density, and LTP, leading to the impairment of synaptic plasticity in the hippocampus. Acupuncture could regulate 14-3-3 expression to improve cognitive function.

Among the 31 DEPs, S100B is the only protein regulating three major processes. S100B is a well-known biomarker for the severity of brain damage and has been shown to predict prognosis after ischemic or traumatic brain injury.<sup>36,37</sup> Increasing evidence has shown that an increase in the synthesis of S100B is positively associated with the neurological deficits,<sup>38,39</sup> whereas S100B inhibitors exert potential neuroprotective effects against cerebral ischemic injuries.<sup>40,41</sup> In our experiment, S100b siRNA was injected into rat lateral ventricle followed by Morris water maze to reveal its role in acupuncture in treating VaD. Results showed that the injection of siRNA targeting S100b had the similar effects to acupuncture on cognition, indicating S100b plays an important role in acupuncture neuroprotective effect.

Among the protein list, there are some proteins which do not belong to the above three functions, such as pannexin-1. Pannexin-1 channels could mediate ATP efflux. Prochnow et al suggested that ATP release through pannexin-1 channels plays a critical role in maintaining synaptic plasticity in CA1 neurons of hippocampus.<sup>42</sup> In addition, our previous study has proven the importance of mitochondrial. In this study, there are a number of mitochondrial proteins identified, such as Tim8, Tim9, and Tom20. However, these proteins differ in the direction of fold differences,

and mitochondrial function is not a significantly biology process in this study. Therefore, the roles of these proteins in acupuncture need further research.

Several studies have demonstrated that the effect of acupuncture on protein expression is dynamic (eg, HMGB1, 14-3-3). In the future research, we will collect samples at different time point after acupuncture for data validation. In addition, our results have shown that S100b plays a vital role in acupuncture neuroprotective effect. It would be worthwhile to further explore the role of S100b-mediated signal pathway in acupuncture treating VaD in our further study.

## 5 | CONCLUSION

In this study, we applied an iTRAQ-based proteomic study to investigate the molecular mechanism for acupuncture on VaD rats. Results suggest that acupuncture improves cognitive function with multifunctional mechanisms of action. These findings help us to get a deeper understanding of the effect of acupuncture on VaD. Finally, the therapeutic efficacy of neuroprotective acupuncture for VaD should be further tested.

## COMPETING INTERESTS

The authors declare no competing financial interests.

## ACKNOWLEDGEMENTS

The study was funded by National Natural Science Foundation of China (Grant No. 81303122).

## ORCID

Cun-Zhi Liu  <http://orcid.org/0000-0001-8031-5667>

## REFERENCES

1. Erkinjuntti T, Roman G, Gauthier S, Feldman H, Rockwood K. Emerging therapies for vascular dementia and vascular cognitive impairment. *Stroke*. 2004;35:1010-1017.
2. Jellinger KA. Morphologic diagnosis of "vascular dementia" - a critical update. *J Neurol Sci*. 2008;270:1-12.
3. Kalaria RN, Maestre GE, Arizaga R, et al. Alzheimer's disease and vascular dementia in developing countries: prevalence, management, and risk factors. *Lancet Neurol*. 2008;7:812-826.
4. Erkinjuntti T, Kurz A, Gauthier S, Bullock R, Lilienfeld S, Damaraju CV. Efficacy of galantamine in probable vascular dementia and Alzheimer's disease combined with cerebrovascular disease: a randomised trial. *Lancet*. 2002;359:1283-1290.
5. Roman GC, Salloway S, Black SE, et al. Randomized, placebo-controlled, clinical trial of donepezil in vascular dementia: differential effects by hippocampal size. *Stroke*. 2010;41:1213-1221.
6. Peng WN, Zhao H, Liu ZS, Wang S. Acupuncture for vascular dementia. *Cochrane Database Syst Rev*. 2007;CD004987.
7. Zeng BY, Zhao K. Effect of acupuncture on the motor and nonmotor symptoms in parkinson's disease—a review of clinical studies. *CNS Neurosci Ther*. 2016;22:333-341.



8. Shi GX, Liu CZ, Guan W, et al. Effects of acupuncture on Chinese medicine syndromes of vascular dementia. *Chin J Integr Med.* 2014;20:661-666.
9. Shi GX, Li QQ, Yang BF, et al. Acupuncture for vascular dementia: a pragmatic randomized clinical trial. *Sci World J.* 2015;2015:161439.
10. Wang XR, Shi GX, Yang JW, et al. Acupuncture ameliorates cognitive impairment and hippocampus neuronal loss in experimental vascular dementia through Nrf2-mediated antioxidant response. *Free Radic Biol Med.* 2015;89:1077-1084.
11. Ye Y, Zhu W, Wang XR, et al. Mechanisms of acupuncture on vascular dementia-A review of animal studies. *Neurochem Int.* 2017;107:204-210.
12. Lin D, Wu Q, Lin X et al. Brain-derived neurotrophic factor signaling pathway: modulation by acupuncture in telomerase knockout mice. *Altern Ther Health Med.* 2015;21(6):36-46.
13. Lin D, De LaPena I, Lin L, Zhou SF, Borlongan CV, Cao C. The neuroprotective role of acupuncture and activation of the BDNF signaling pathway. *Int J Mol Sci.* 2014;15:3234-3252. <https://doi.org/10.3390/ijms15023234>
14. Ross PL, Huang YN, Marchese JN, et al. Multiplexed protein quantitation in *Saccharomyces cerevisiae* using amine-reactive isobaric tagging reagents. *Mol Cell Proteomics.* 2004;3:1154-1169.
15. Wu WW, Wang G, Baek SJ, Shen RF. Comparative study of three proteomic quantitative methods, DIGE, cICAT, and iTRAQ, using 2D gel- or LC-MALDI TOF/TOF. *J Proteome Res.* 2006;5:651-658.
16. Jia Y, Jin W, Xiao Y, et al. Lipoxin A4 methyl ester alleviates vascular cognition impairment by regulating the expression of proteins related to autophagy and ER stress in the rat hippocampus. *Cell Mol Biol Lett.* 2015;20:475-487.
17. Luo P, Chen C, Lu Y, et al. Baclofen ameliorates spatial working memory impairments induced by chronic cerebral hypoperfusion via up-regulation of HCN2 expression in the PFC in rats. *Behav Brain Res.* 2016;308:6-13.
18. Ye Y, Li H, Yang JW, et al. Acupuncture attenuated vascular dementia-induced hippocampal long-term potentiation impairments via activation of D1/D5 receptors. *Stroke.* 2017;48(4):1044-1051.
19. Williams KE, Miroshnychenko O, Johansen EB, et al. Urine, peritoneal fluid and omental fat proteomes of reproductive age women: Endometriosis-related changes and associations with endocrine disrupting chemicals. *J Proteomics.* 2015;113:194-205.
20. O'Brien JT, Thomas A. Vascular dementia. *Lancet.* 2015;386:1698-1706.
21. Khan A, Kalaria RN, Corbett A, Ballard C. Update on vascular dementia. *J Geriatr Psychiatry Neurol.* 2016;29:281-301.
22. Zhu Y, Zeng Y. Electroacupuncture protected pyramidal cells in hippocampal CA1 region of vascular dementia rats by inhibiting the expression of p53 and Noxa. *CNS Neurosci Ther.* 2011;17:599-604.
23. Zhu Y, Wang X, Ye X, Gao C, Wang W. Effects of electroacupuncture on the expression of p70 ribosomal protein S6 kinase and ribosomal protein S6 in the hippocampus of rats with vascular dementia. *Neural Regen Res.* 2012;7:207-211.
24. Zhu Y, Zeng Y, Wang X, Ye X. Effect of electroacupuncture on the expression of mTOR and eIF4E in hippocampus of rats with vascular dementia. *Neurosci.* 2013;34:1093-1097.
25. Lin L, Skakavac N, Lin X et al. Acupuncture-Induced Analgesia: The Role of Microglial Inhibition. *Cell Transplant.* 2016;25(4):621-628. <https://doi.org/10.3727/096368916X690872>.
26. Li H, Liu Y, Lin LT, et al. Acupuncture reversed hippocampal mitochondrial dysfunction in vascular dementia rats. *Neurochem Int.* 2016;92:35-42.
27. Shi GX, Wang XR, Yan CQ, et al. Acupuncture elicits neuroprotective effect by inhibiting NADPH oxidase-mediated reactive oxygen species production in cerebral ischaemia. *Sci Rep.* 2015;5:17981.
28. Li Z, Wang Y, Xie Y, Yang Z, Zhang T. Protective effects of exogenous hydrogen sulfide on neurons of hippocampus in a rat model of brain ischemia. *Neurochem Res.* 2011;36:1840-1849.
29. Spranger M, Kremien S, Schwab S, Donneberg S, Hacke W. Superoxide dismutase activity in serum of patients with acute cerebral ischemic injury. Correlation with clinical course and infarct size. *Stroke.* 1997;28:2425-2428.
30. Jung JE, Kim GS, Narasimhan P, Song YS, Chan PH. Regulation of Mn-superoxide dismutase activity and neuroprotection by STAT3 in mice after cerebral ischemia. *J Neurosci.* 2009;29:7003-7014.
31. Lin R, Lin Y, Tao J, et al. Electroacupuncture ameliorates learning and memory in rats with cerebral ischemia-reperfusion injury by inhibiting oxidative stress and promoting p-CREB expression in the hippocampus. *Mol Med Rep.* 2015;12:6807-6814.
32. Qi L, Sun X, Li FE, et al. HMGB1 Promotes Mitochondrial Dysfunction-Triggered Striatal Neurodegeneration via Autophagy and Apoptosis Activation. *PLoS One.* 2015;10:e0142901.
33. Ding HS, Yang J, Gong FL, et al. High mobility group [corrected] box 1 mediates neutrophil recruitment in myocardial ischemia-reperfusion injury through toll like receptor 4-related pathway. *Gene.* 2012;509:149-153.
34. Malenka RC. Synaptic plasticity in the hippocampus: LTP and LTD. *Cell.* 1994;78(4):535-538.
35. Simsek-Duran F, Linden DJ, Lonart G. Adapter protein 14-3-3 is required for a presynaptic form of LTP in the cerebellum. *Nat Neurosci.* 2004;7:1296-1298.
36. Foerch C, Singer OC, Neumann-Haefelin T et al. Evaluation of serum S100B as a surrogate marker for long-term outcome and infarct volume in acute middle cerebral artery infarction. *Arch Neurol.* 2005;62:1130-1134.
37. Savola O, Pyhtinen J, Leino TK, Siitonen S, Niemelä O, Hillbom M. Effects of head and extracranial injuries on serum protein S100B levels in trauma patients. *J Trauma.* 2004;56:1229-1234.
38. Mori T, Asano T, Town T. Targeting S100B in Cerebral Ischemia and in Alzheimer's Disease. *Cardiovasc Psychiatry Neurol.* 2010.
39. Mori T, Tan J, Arendash GW, Koyama N, Nojima Y, Town T. Overexpression of human S100B exacerbates brain damage and periinfarct gliosis after permanent focal ischemia. *Stroke.* 2008;39:2114-2121.
40. Mori T, Town T, Tan J, Tateishi N, Asano T. Modulation of astrocytic activation by arundic acid (ONO-2506) mitigates detrimental effects of the apolipoprotein E4 isoform after permanent focal ischemia in apolipoprotein E knock-in mice. *J Cereb Blood Flow Metab.* 2005;25:748-762.
41. Yang J, Song TB, Zhao ZH, Qiu SD, Hu XD, Chang L. Vasoactive intestinal peptide protects against ischemic brain damage induced by focal cerebral ischemia in rats. *Brain Res.* 2011;1398:94-101.
42. Prochnow N, Abdulazim A, Kurtenbach S, et al. Pannexin 1 stabilizes synaptic plasticity and is needed for learning. *PLoS One.* 2012;7:e51767.

## SUPPORTING INFORMATION

Additional supporting information may be found online in the Supporting Information section at the end of the article.

**How to cite this article:** Yang J-W, Wang X-R, Zhang M, et al. Acupuncture as a multifunctional neuroprotective therapy ameliorates cognitive impairment in a rat model of vascular dementia: A quantitative iTRAQ proteomics study. *CNS Neurosci Ther.* 2018;00:1-11. <https://doi.org/10.1111/cns.13063>